

LA-1214

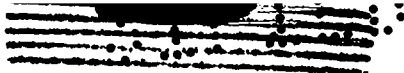
SEP 18 19 20

Series A

LOS ALAMOS NATIONAL LABORATORY



3 9338 00419 5748



UNCLASSIFIED

LOS ALAMOS SCIENTIFIC LABORATORY

of

THE UNIVERSITY OF CALIFORNIA

PUBLICLY RELEASABLE

3 February 1951

Per M. Pankratz, FSS-16 Date: 11-16-95 LA-1214

By James J. DeB., CIC-14 Date: 12-19-95

This Document Consists of 44 Pages



Classification changed to **UNCLASSIFIED**
by authority of the U. S. Atomic Energy Commission.

Per ALDR(TID-1400-S2) Sept.-Oct 1974

By **REPORT LIBRARY** Adm. Monitoring, 3/17/75

RATE OF GROWTH OF ATOMIC FIREBALLS

VERIFIED UNCLASSIFIED

Per LNR 6/20/79

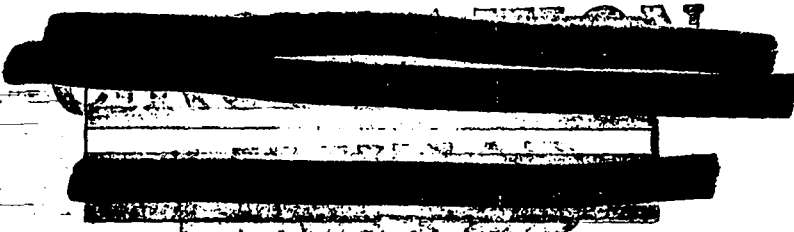
By James J. DeB. 12/19/95

Work Done By:

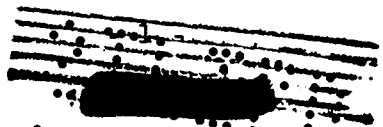
Francis B. Porzel

Report Written By:

Francis B. Porzel



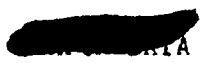
LOS ALAMOS NATL. LAB. LIBS.
3 9338 004 19 5748



010614K1259
UNCLASSIFIED

SECRET

UNCLASSIFIED



APR 16 1951
April 3, 1951

LA-1214

Washington Document Room
J R. Oppenheimer
Los Alamos Document Room

1 thru 4
5
6 thru 20



UNCLASSIFIED


UNCLASSIFIEDABSTRACT

Previous theory predicted that the radius of the fireball should vary as the 0.4 power of the time from detonation. In the present work, the growth of the fireball is derived principally from the theory of strong shocks, but the equations of motion include two factors which have been previously neglected: first, an early phase of the explosion, where strong shock theory is not applicable, during which transport of energy by radiation is used as a model, and second, the variation in γ , the ratio of specific heats. The equation of motion is integrated; the result is a "predicted" radius vs time curve with a variable power of time whose average value is approximately 0.377 over the range of measurement. This is in excellent agreement with the observed results from Sandstone, 0.374 ± 0.005 .


UNCLASSIFIED



UNCLASSIFIED

RATE OF GROWTH OF ATOMIC FIREBALLS

1. PURPOSE

It was a well-known result from simple theory of strong shocks that the radius of the fireball should vary as the 2/5 power of the time from detonation, i.e.,

$$R = \text{constant} \times t^{0.4}$$

Repeated measurements of fireball growth at Sandstone have not verified this exponent as 0.4, but rather as 0.374 ± 0.005 . The purpose of this paper is to examine the fireball growth more closely, this in order to (1) determine whether significant departures from the 0.4 law are reasonable; (2) predict, if possible, an expected radius vs time curve; and (3) suggest, on this basis, appropriate methods of scaling bombs of different yields.

2. DERIVATION OF A RADIUS VS TIME CURVE

2.1 Deficiencies in the 0.4 Law

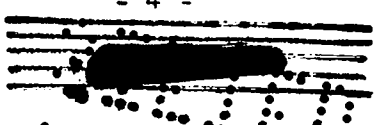
The considerations that lead to the 0.4 law were from strong shock theory which showed that

$$U \sim P^{1/2}$$

where

- U = shock velocity
- P = pressure

Handwritten notes:
 $U \sim P^{1/2}$
 $U = U_s (1 - \frac{U}{U_s})$
 $P = P_0 U_s U P$
 $P = P_0 U_s^2 (1 - \frac{U}{U_s})^2$



UNCLASSIFIED

UNCLASSIFIED

and from similarity conditions,

$$P \sim 1/R^3,$$

where

R = radius of shock front.

Therefore,

$$U = \frac{dR}{dt} \sim \frac{1}{R^{3/2}}$$

and

$$R \sim t^{2/5}.$$

It is this derivation which will be critically examined.

The radius of the shock front is more precisely given by the definitions

$$R = \int_0^t \frac{dR}{dt} dt = \int_0^t U dt,$$

or conversely,

$$t = \int_0^R \frac{dt}{dR} dR = \int_0^R \frac{dR}{U}.$$

UNCLASSIFIED

~~UNCLASSIFIED~~

At the outset, it should be noted that one cannot accurately know $R = F(t)$ unless $U(R)$ or $U(t)$ is known over the entire range of integration from zero time. Two weaknesses in the assumptions on which the 0.4 law is derived are apparent. First, strong shock theory is seriously perturbed, if not inapplicable, during the first few meters of growth, because of radiative effects and the finite mass of the bomb itself. Second, unless U is of the form $U = \text{constant} \times P^n$, where n is constant, then the integration leads to a more complex result, depending, of course, on the form of $U = F(P)$. The 0.4 law is suspect here because of variation in γ , the ratio of specific heats.

A complete derivation should recognize three phases of fireball growth:

$$t = \int_0^{\text{Edge of bomb case}} \frac{dt}{dR} dR + \int_{\text{Edge of case}}^{\text{Beginning of true shock}} \frac{dt}{dR} dR + \int_{\text{Beginning of true shock}}^t \frac{dt}{dR} dR .$$

We will neglect the first of these integrals as too small, and because its effect, if any, could be consolidated with the second integral. We refer to the second integral as the "radiative" phase and to the third integral as the "strong shock" phase. It will be simpler to discuss these in reverse order, strong shock before radiation.

UNCLASSIFIED

2.2 Strong Shock Theory with Variable Gamma

Solely by conservation of mass and momentum, the Rankine-Hugoniot equations give the shock velocity as

$$U^2 = \frac{(P - P_0)}{(V_0 - V)} V_0^2,$$

where

P, P_0 = pressure behind and ahead of the shock

V, V_0 = specific volumes.

In the air ahead of the shock, specify the sound velocity as C_0 and the ratio of specific heats as γ_0 ; the relation

$$C_0 = \sqrt{\gamma_0 P_0 V_0}$$

holds, independently of any consideration of variable γ .

We define

$$\xi = P/P_0,$$

with the result that

$$U^2 = P_0 V_0 \frac{(\xi - 1)}{\left(1 - \frac{V}{V_0}\right)} = \frac{C_0^2}{\gamma_0} \frac{(\xi - 1)}{\left(1 - \frac{V}{V_0}\right)}. \quad (1)$$

UNCLASSIFIED

UNCLASSIFIED

In the usual treatment, γ is assumed constant. From the Rankine-Hugoniot energy relations,

$$\frac{V}{V_0} = \frac{(\gamma - 1) P + (\gamma + 1) P_0}{(\gamma + 1) P + (\gamma - 1) P_0}$$

For $P \gg P_0$,

$$\frac{V}{V_0} = \frac{\gamma - 1}{\gamma + 1},$$

$$\frac{P}{P_0} = \frac{\gamma + 1}{\gamma - 1} = 2\gamma - 2$$

$$\gamma = 3$$

$$\frac{V}{V_0} = \frac{1}{6} \quad \text{for } \gamma = 1.4.$$

From these considerations, and from the assumption that $(\gamma - 1)$ is small, Fuchs gave the result that for strong shocks,

$$U^2 = c_0^2 \xi$$

For very strong shocks, however, $(\gamma - 1)$ is neither negligible nor a constant. The variability of γ has been previously considered by the author in an unpublished paper. For present purposes, define a γ such that

$$\text{Internal Energy} = E_1 = \frac{P V}{\gamma - 1} \quad (2)$$

UNCLASSIFIED

UNCLASSIFIED

The advantage in this is to substitute a slowly-varying function, γ , for a rapidly varying function like E ; γ_0 is, of course, 1.4. The Rankine-Hugoniot energy relationship becomes

$$E - E_0 = \frac{1}{2} (P + P_0)(V_0 - V) = \frac{P V}{\gamma - 1} - \frac{P_0 V_0}{\gamma_0 - 1} .$$

After algebraic transformation, this becomes

$$\frac{V}{V_0} = \frac{\gamma - 1}{\gamma_0 - 1} \left[\frac{(\gamma_0 - 1) P + (\gamma_0 + 1) P_0}{(\gamma + 1) P + (\gamma - 1) P_0} \right] .$$

Replacing P/P_0 by ξ , and setting $\gamma_0 = 1.4$,

$$\frac{V}{V_0} = \frac{\xi + 6}{\left(\frac{\gamma+1}{\gamma-1}\right) \xi - 1} . \quad (3)$$

For $\xi \gg 6$, this reduces to an expression similar to that for constant γ ,

$$\frac{V}{V_0} = \frac{\gamma - 1}{\gamma + 1} ,$$

except that here V/V_0 does not approach a constant limit, but is a function of the shock strength ξ .

UNCLASSIFIED

UNCLASSIFIED

We do not require the strong condition that $\xi \gg 6$;
instead, the weaker condition

$$\xi \gg \left(\frac{\gamma - 1}{2} \right)^2$$

leads to

$$1 - \frac{v}{v_0} = \frac{2}{\gamma + 1} .$$

In this approximation, Eq. 1 becomes

$$u^2 = \frac{c_0^2}{\gamma_0} \frac{\gamma + 1}{2} (\xi - 1)$$

$$\approx c_0^2 \xi \frac{\gamma + 1}{2\gamma_0} , \quad \xi \gg 1. \quad (4)$$

This is a more accurate form than $u^2 = c_0^2 \xi$, in that it allows for the variation in γ .

The shape of a radius vs time curve depends basically on this equation. The problem is to integrate the equation of motion.

UNCLASSIFIED



The dependence of γ on ξ was found using the definition in Eq. 2 and the resulting Rankine-Hugoniot relations set forth in Eq. 3.¹ The results are given in Fig. 1; note in particular the minimum value of γ at approximately 700 atmospheres.

2.3 Evaluation of the Time Integrand During Strong Shock Phase

We evaluate the time integral during the shock phase, and upon these results will base the accuracy required for the radiative phase.

Given

$$\frac{dR}{dt} = \frac{C_0}{\sqrt{2\gamma_0}} (\xi - 1)^{1/2} (\gamma + 1)^{1/2}$$

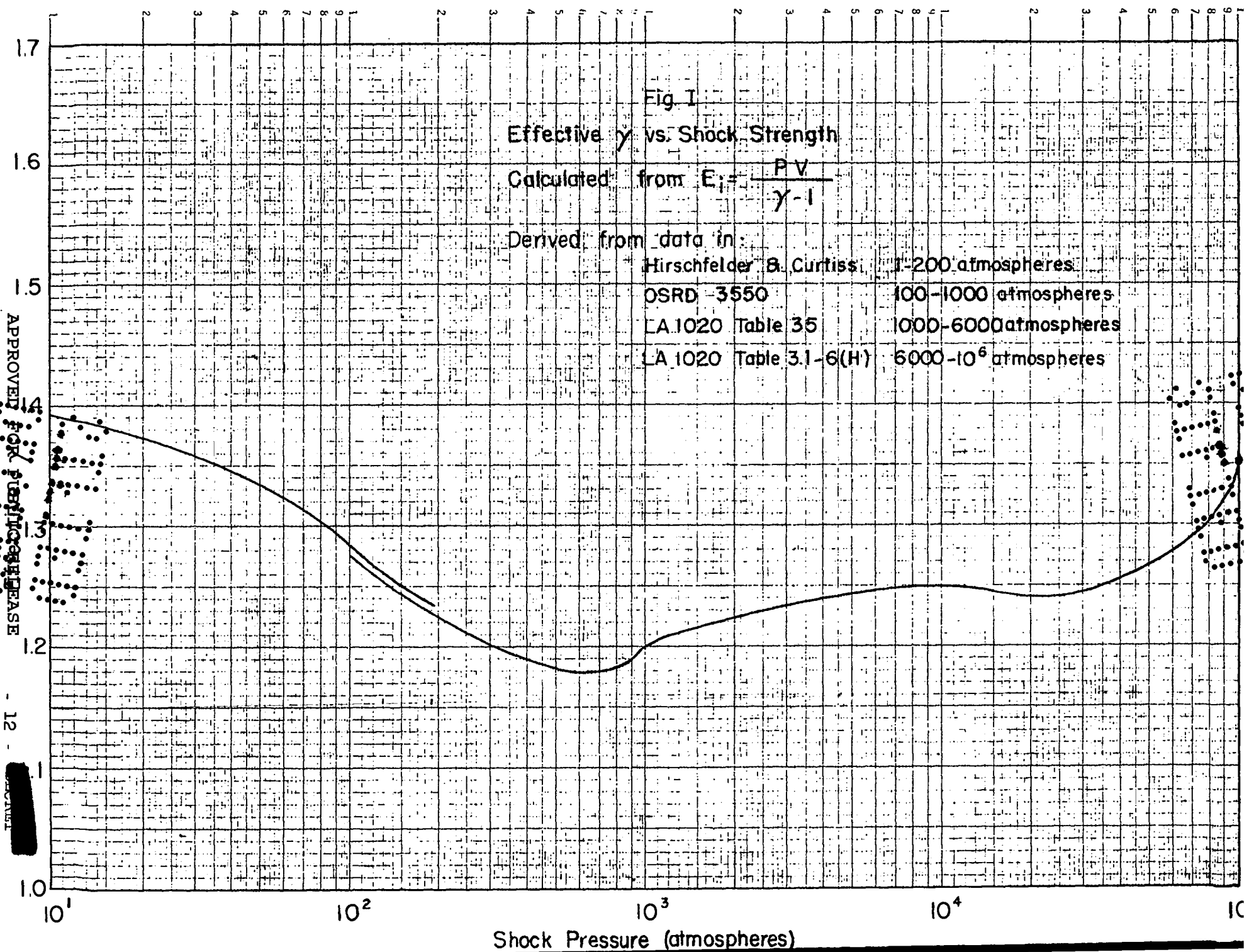
we can integrate provided we know $\xi = \xi(R)$, because we now know $\gamma = \gamma(\xi)$. It is preferable to integrate as

¹

The actual computations were done by C. H. Maker while he was a member of the J.7 Blast Measurements Sub-Group. Three sources of data were used to furnish the necessary equations of state and values of $V/V_0 = F(\xi)$:

- (a) C. F. Curtiss and J. O. Hirschfelder, "Thermodynamic Properties of Air", NOrd 9938, Task Wis-1-A, 1 June 1948.
- (b) S. R. Brinkley, J. G. Kirkwood, J. M. Richardson, "Properties of Air Along a Hugoniot Curve", OSRD 3550, 27 April 1944.
- (c) K. Fuchs, R. E. Peierls, "The Equation of State of Air", LA-1020, Chap. 3, 6 April 1948.





Shock Pressure (atmospheres)

$$t = \int \frac{dt}{dR} dR = \frac{\sqrt{2\gamma_0}}{c_0} \int \frac{dR}{(\xi - 1)^{1/2}} (\gamma + 1)^{1/2},$$

because ξ is more easily expressed as $\xi(R)$ than $\xi(t)$, and the integrand $\rightarrow 0$, as $\xi \rightarrow \infty$.

The usual form for $\xi(R)$ is obtained from dimensional considerations and for strong shocks is

$$\frac{P}{P_0} = \frac{A}{\left(\frac{R}{W^{1/3}}\right)^3} = \frac{WA}{R^3}.$$

where

P = overpressure behind the shock

W = energy of blast

A = constant.

Now

$$\xi = \frac{P}{P_0} + 1$$

or

$$(\xi - 1) = \frac{WA}{R^3}.$$

We do not choose to question the inverse cube law at present, nor can we specify A exactly. The integral becomes

$$t = \frac{\sqrt{2\gamma_0}}{c_0 (WA)^{1/2}} \int \frac{R^{3/2} dR}{(\gamma + 1)^{1/2}} \quad (5)$$

The coefficient A may be roughly determined from Sandstone fireball data and from extrapolation of peak-pressure measurements. Such a calculation and a comparison of results are given in Appendix A.

For the integration, an arbitrary tonnage was selected such that

$$WA = 6 \times 10^6 .$$

(From the considerations in Appendix A, the approximate tonnage of the bomb is 1.5 kt.) The integrand was then tabulated as a function of ξ , and the corresponding value of R determined from

$$\begin{aligned} R &= \left(\frac{WA}{\xi} \right)^{1/3} \\ &= \left(\frac{6 \times 10^6}{\xi} \right)^{1/2} . \end{aligned}$$

We have, then, that

$$\frac{dt}{dR} = \frac{\sqrt{2\gamma_0}}{c_0} \left(\sqrt{6 \times 10^6} \right) \frac{R^{3/2}}{(\gamma + 1)^{1/2}} .$$

In arbitrary time units, the function

$$\frac{dt}{dR} = \frac{R^{3/2}}{(\gamma + 1)^{1/2}}$$

is tabulated in Table 1 and plotted in Fig. 2. Two values of dt/dR are shown, the actual value,

$$\frac{R^{3/2}}{(\gamma + 1)^{1/2}},$$

and for comparison,

$$\frac{R^{3/2}}{1.52}.$$

The latter corresponds to dt/dR for constant $\gamma = 1.31$, which applies to pressures of 70 atmospheres near the end of the fireball measurements, and to pressures of 80,000 atmospheres somewhat below the beginning of fireball measurements. This was a convenient "best fit" of a 0.4 law to the predicted dt/dR curve; it furnishes a convenient base for later integration and is in itself instructive. The curves match at both pressures; this means that at both points, the velocity is matched by the best possible fit from a single 0.4 law. But the variation in γ in the integrand affects the radius-time plot by making an S-shaped curve as indicated in Fig. 3.



TABLE 1

dt/dR as Function of R

ξ	γ	$\sqrt{\gamma+1}$	$\frac{WA}{\xi}$	$R^{3/2}$	$\frac{R^{3/2}}{\sqrt{\gamma+1^{1/2}}}$	$\frac{R^{3/2}}{1.52}$	$\Delta \frac{dt}{dR}$	R
150,000	1.372	1.54	40	6.31	4.10	4.15		3.42
100,000	1.325	1.525	60	7.75	5.08	5.10		3.91
80,000	1.300	1.516	75	8.66	5.71	5.69		4.21
50,000	1.277	1.508	120	10.95	7.26	7.21		4.93
40,000	1.255	1.500	150	12.25	8.27	8.06		5.31
20,000	1.241	1.497	300	17.32	11.60	11.39	0.21	6.69
10,000	1.250	1.500	600	24.48	16.32	16.10	0.22	8.43
6,000	1.249	1.499	1,000	31.62	21.09	20.80	0.29	10.00
5,000	1.245	1.498	1,200	34.64	23.12	22.79	0.33	10.62
4,000	1.240	1.497	1,500	38.73	25.87	25.48	0.39	11.45
3,000	1.232	1.494	2,000	44.72	29.93	29.42	0.51	12.60
2,000	1.221	1.491	3,000	54.77	36.73	36.03	0.70	14.42
1,000	1.220	1.483	6,000	77.46	52.23	50.96	1.63	18.17
900	1.190	1.480	6,660	81.61	55.14	53.69	1.45	18.80
800	1.183	1.477	7,500	86.60	58.63	56.97	1.65	19.56
700	1.179	1.476	8,580	92.64	62.75	60.95	1.80	20.42
600	1.179	1.476	10,000	100.0	67.75	65.79	1.96	21.54
500	1.184	1.479	12,000	109.6	74.10	72.10	2.00	22.80
400	1.191	1.480	15,000	122.5	82.77	80.59	2.18	24.66
300	1.202	1.483	20,000	141.4	95.34	93.02	2.32	27.14
200	1.222	1.491	30,000	173.2	116.2	113.9	2.3	31.07
150	1.245	1.498	40,000	200.0	133.5	131.6	1.9	34.20
100	1.283	1.511	60,000	244.9	162.1	161.0	1.1	39.15
90	1.292	1.514	66,600	258.0	170.4	169.7	0.7	40.50
80	1.302	1.517	75,000	273.9	180.6	180.2	0.4	42.30
70	1.311	1.521	85,800	292.9	192.5	192.7	- 0.1	44.10
60	1.321	1.524	100,000	316.2	207.5	208.0	- 0.5	46.42
50	1.332	1.527	120,000	346.4	226.9			49.32
40	1.345	1.531	150,000	387.3	253.0			53.13

Radiative Phase

	dt/dR	R
By fitting →	5.69	4.21
to strong shock	5.24	4.0
phase at	4.84	3.8
R = 4.21	4.45	3.6
	3.40	3.0
	2.6	2.5



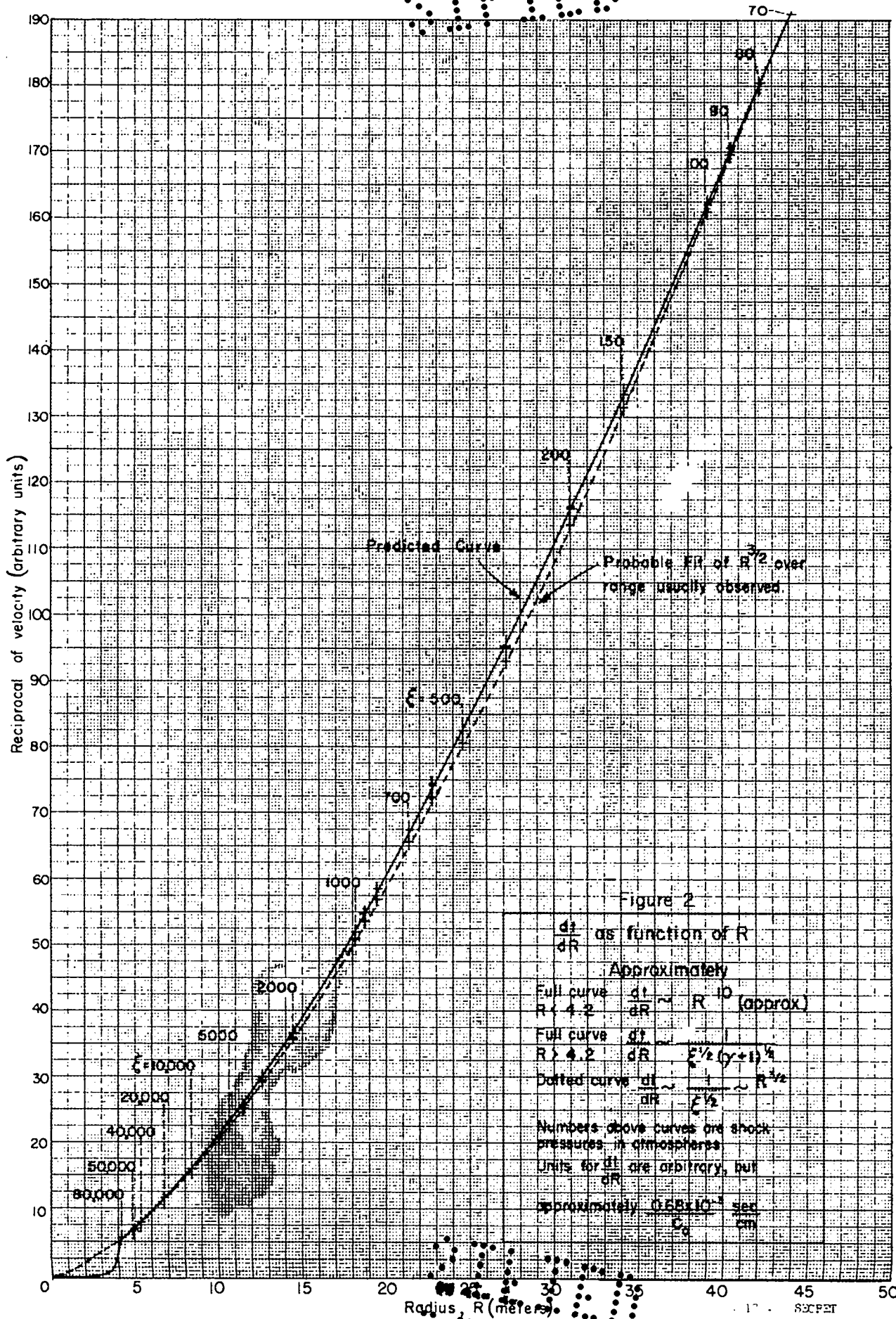


Figure 2

$\frac{dt}{dR}$ as function of R

Approximately

Full curve $\frac{dt}{dR} \sim R^{-10}$ (approx)

Full curve $\frac{dt}{dR} \sim \frac{1}{R^{1/2}(\gamma+1)^2}$

Dotted curve $\frac{dt}{dR} \sim \frac{1}{C^2} \sim R^{-3/2}$

Numbers above curves are shock pressures in atmospheres

Units for $\frac{dt}{dR}$ are arbitrary, but

approximately $0.68 \times 10^{-3} \frac{\text{sec}}{\text{cm}}$

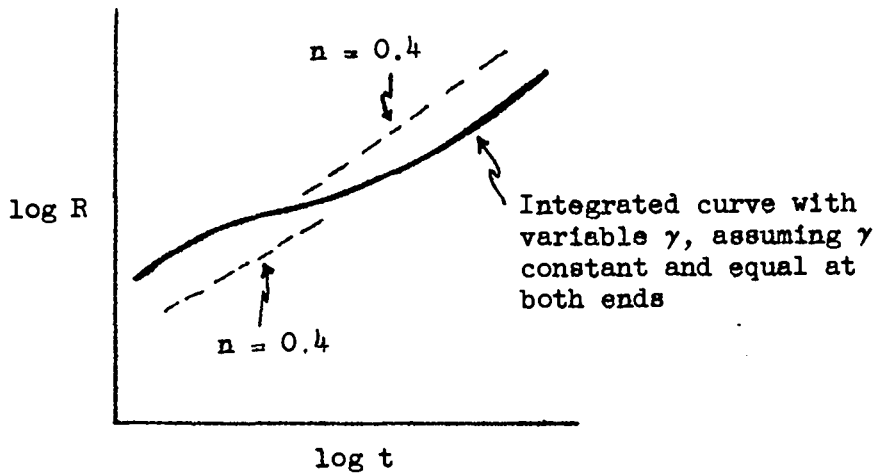


Fig. 3

Effect of the Variation in γ on the Radius-Time Plot

The point is that the whole range of low values of γ in the region of interest contribute to the displacement of the S curve. If the pressure range considered encompassed the whole range from 10^7 atmospheres ($\gamma = 1.67$) down to 10 atmospheres ($\gamma = 1.4$), the distortion would be much larger. By itself, the variation in γ is not sufficient to explain the entire deviation from the 0.4 law; over the range of pressures considered here, it would reduce the average slope to perhaps 0.395. At small enough radii, the strong shock conditions are no longer applicable in any case.



2.4 Evaluation of the Time Integrand During the Radiative Phase

The purpose of this section is to show by a convenient model that a serious deviation from strong shock theory at very low radii will distort the radius-time curve at much later times. The precise nature of the dt/dR curve in this region is not decisive; what matters is whether or not there is a period during which energy has been transported outward faster than predicted by the 0.4 law.

The radiative phase has been described by Hirschfelder and Magee;² their description appears to be sufficient for present purposes. When the explosion reaches the edge of the case, the temperature is so high that radiation, rather than shock, presents the most rapid mechanism of energy transfer. For a 10-kt bomb, they show that a sharp transition from a "radiative front" to a shock front occurs between radii of 5 and 10 meters, the radiation front being initially much faster than the shock front. This condition continues until the temperature drops to about $300,000^{\circ}$ K, when the shock can actually overtake the radiation front.

The criterion of $300,000^{\circ}$ K corresponds to a pressure of 80,000 atmospheres, and for the bomb we are considering, occurs at 4.2 meters. (It is also the pressure at which we had matched the strong shock integrands.) An inspection of Fig. 2 shows that the exact form of dt/dR below 4 meters is not very important at $R = 10$ meters.

² J. Hirschfelder, J. Magee, "Radiation Phenomena in Air Blast of Gadget", LA-1020, Vol. 7, Chap. 4, 6 April 1948.





Accordingly, the following dimensional analysis is probably satisfactory.

In this region, the mean free path of radiation is

$$\lambda \sim T^3,$$

where

T = absolute temperature.

If one visualizes the mechanism of radiation transport as that of successive capture and delayed emission of quanta, then the velocity of radiation, V , is given by

$$V \sim \lambda.$$

For instantaneous emission and spherical geometry, we have³

$$x \sim \lambda \sqrt{n}$$

$$t \sim \frac{n \lambda}{c}$$

$$V = \frac{x}{t} = \frac{c}{\sqrt{n}},$$

where

x = distance travelled

n = number of collisions

³

This correction was pointed out by F. Reines and B. R. Suydam.





t = time required

c = velocity of light.

But

$$\sqrt{n} \sim \frac{x}{\lambda} ,$$

so that

$$v \sim \frac{c \lambda}{x} .$$

For an isothermal sphere, we have that

Total Energy = Constant \sim Volume \times Temperature,

$$\therefore T \sim \frac{1}{R^3} .$$

From this, it follows that

$$v = \frac{dR}{dt} \sim \frac{\lambda}{R} \sim \frac{T^3}{R} \sim \frac{1}{R^{10}} .$$

The radius-time relationship for the radiation front is of the form

$$R \sim \frac{1}{t^{11}} .$$

This, in itself, is sufficient to indicate that the dt/dR curve rises very sharply near the critical radius of shock catch-up.

The procedure used was to plot the function





$$\frac{dt}{dR} = \frac{1}{V} = K R^9,$$

where K is chosen to make these curves match at $R = 4.2$.

The tabulated values for dt/dR during the radiative phase are included in Table 1 and plotted in Fig. 2.

2.5 Evaluation of the Time Integral: Final Results

The differences between the predicted curve and a 0.4 law were known to be small, and the $R^{3/2}/1.52$ was fitted to keep the differences as small as possible. This permits a special graphical integration with a high order of accuracy.

The integral for the 0.4 law,

$$t = \int \frac{R^{3/2}}{1.52} dR,$$

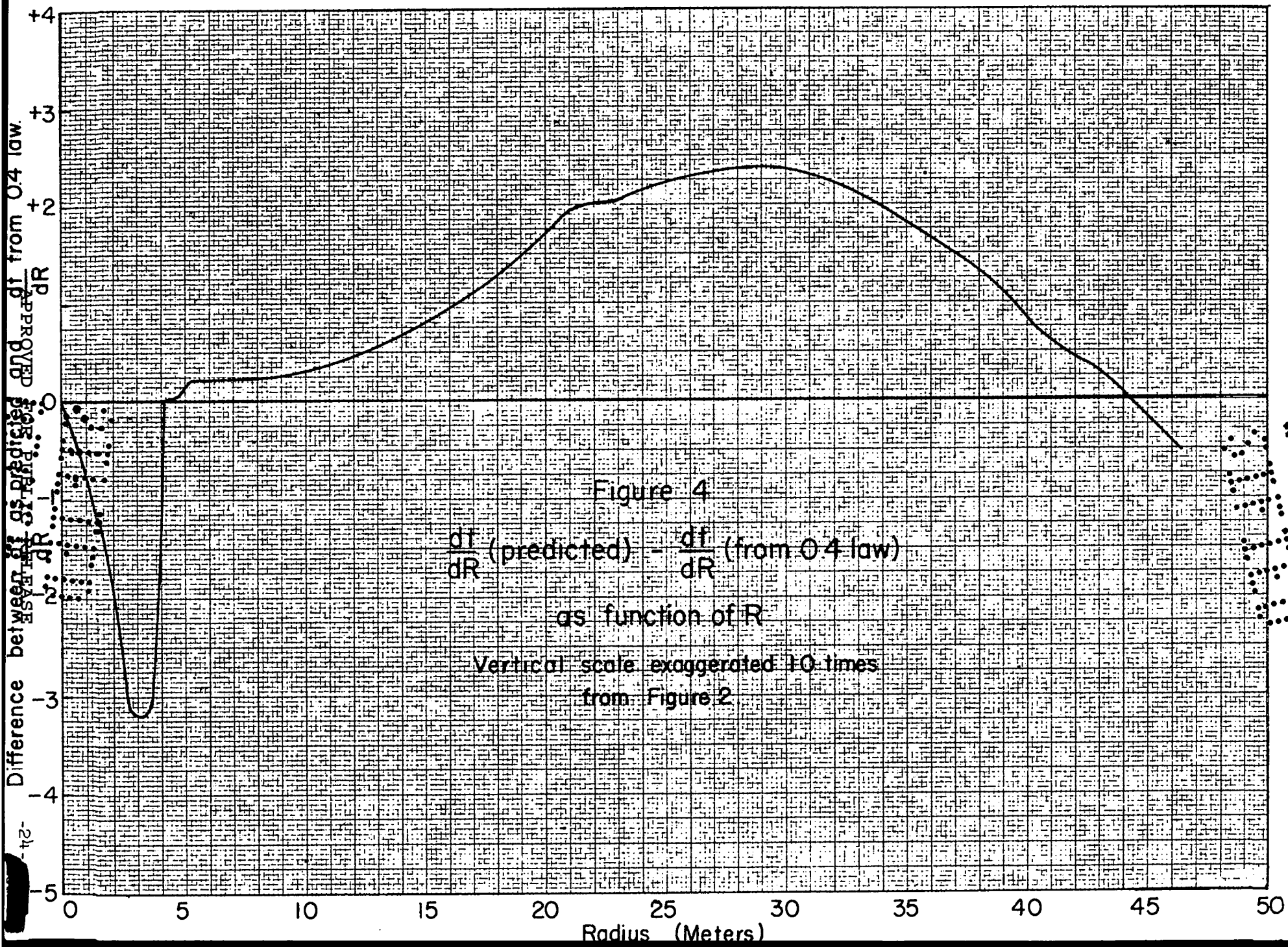
was calculated and is given in Column 4 of Table 2. From Table 1, the difference in dt/dR between the 0.4 law and the predicted curve was calculated (Column 8, Table 1). The difference was exaggerated ten times and is plotted as a function of R in Fig. 4. This curve was then integrated with a planimeter and the result is a time correction, Δt , given in Fig. 5 and Column 2, Table 2, which is applied to the corresponding time for a 0.4 law. Analytically, the procedure followed is given by the equation,



TABLE 2

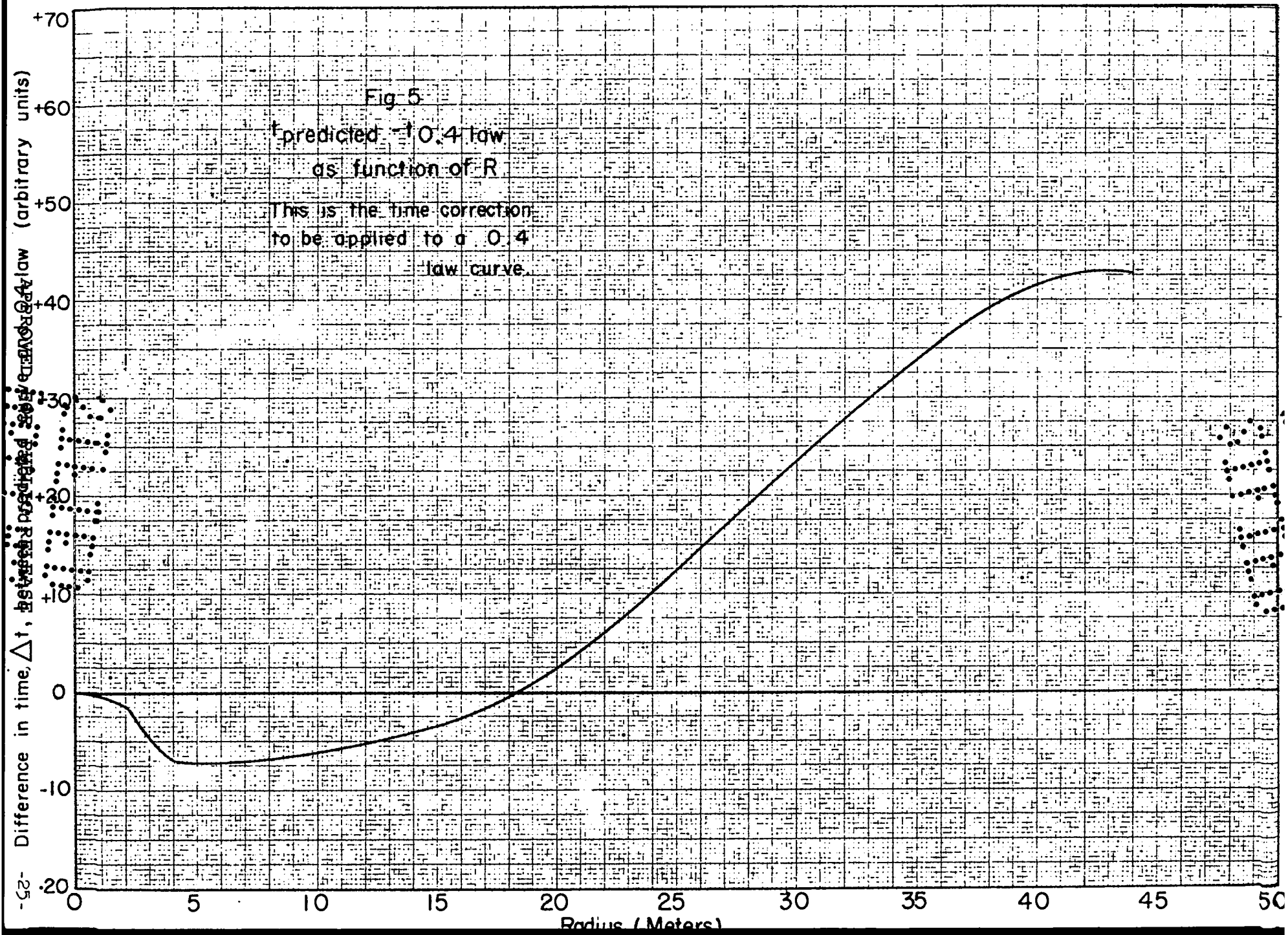
t and n as Functions of R

R (meters)	Δt (arbitrary units)	$R^{5/2}$	t 0.4 law (arbitrary units)	t (arbitrary units)	$\frac{R_{n+1}}{R_n}$	$\frac{t_n}{t_{n+1}}$	n	t 0.4 law (ms)	t predicted (ms)
0	- 1.49						0.091		
2		5.66	1.49	---			0.091	0.0030	
3	- 4.03	15.59	4.10	0.06			0.091	0.0082	0.00012
4.2	- 7.09	36.15	9.51	2.40	1.429	6.821	0.187	0.0190	0.0048
6	- 6.83	88.18	23.20	16.37	1.333	2.516	0.311	0.0464	0.0327
8	- 6.45	181.04	47.64	41.19	1.500	3.063	0.362	0.0953	0.0824
12	- 5.05	498.8	131.26	126.2	1.333	2.116	0.382	0.263	0.252
16	- 2.49	1024	269.46	267.0	1.250	1.774	0.389	0.539	0.534
20	+ 2.81	1789	470.77	473.6	1.250	1.762	0.394	0.942	0.947
25	+ 12.4	3125	822.3	834.7	1.200	1.583	0.397	1.65	1.67
30	+ 24.0	4930	1297.3	1321.3	1.167	1.469	0.402	2.59	2.64
35	+ 34.1	7247	1907.4	1941.5	1.143	1.393	0.406	3.82	3.88
40	+ 41.5	10120	2663.0	2704.5	1.100	1.266	0.404	5.33	5.41
44	+ 43.9	12842	3379.4	3423.3				6.76	6.85



Difference between predicted and 0.4-law

Radius (Meters)



~~SECRET~~


$$\Delta t = \int \left[\frac{dt}{dR} \text{ (predicted)} - \frac{dt}{dR} \text{ (0.4 law)} \right] dR ,$$

$$t_{\text{predicted}} = t_{0.4 \text{ law}} + \Delta t .$$

The values of $t_{\text{predicted}}$ are given in Column 5 of Table 2. During the radiative phase, the difference between the two laws was large and $t_{\text{predicted}}$ was calculated directly from

$$\frac{dt}{dR} = 5.69 \left(\frac{R}{4.2} \right)^{10}$$

$$t = \left(\frac{5.69}{10} \right) 4.2 \left(\frac{R}{4.2} \right)^{11}$$

This also furnished a check point for Δt at $R = 4.2$, where dt/dR changes sign and Δt becomes progressively less negative.

A presentation of results in actual time is tabulated in Columns 9 and 10 of Table 2. The original integral was

$$\frac{dt}{dR} = \sqrt{\frac{2\gamma_0}{C_0}} (WA)^{1/2} \int \frac{R^{3/2}}{(\gamma + 1)^{1/2}} dR ,$$

and until now the time was carried without the constant term, i.e., in arbitrary time units. Actual time is related to the arbitrary time by





$$t_{\text{actual}} = \sqrt{\frac{2\gamma_0}{C_0}} (WA)^{1/2} (t_{\text{arbitrary}})$$

$$C_0 = 0.345 \text{ meters/msec,}$$

$$\gamma_0 = 1.4,$$

$$WA = 6 \times 10^6 .$$

Inserting these values,

$$t_{\text{actual}} = 0.002 t_{\text{arbitrary}}$$

The usual presentation of $\log R$ vs $\log t$ is given in Fig. 6. Three lines are shown: the full line for $t_{\text{predicted}}$, the dotted line for the best fit of a 0.4 law, and for comparison, a slope of 0.375 plotted some distance below. From Fig. 6, the reason is readily apparent for the slope measured on Sandstone, and 0.374 is indeed an excellent fit.

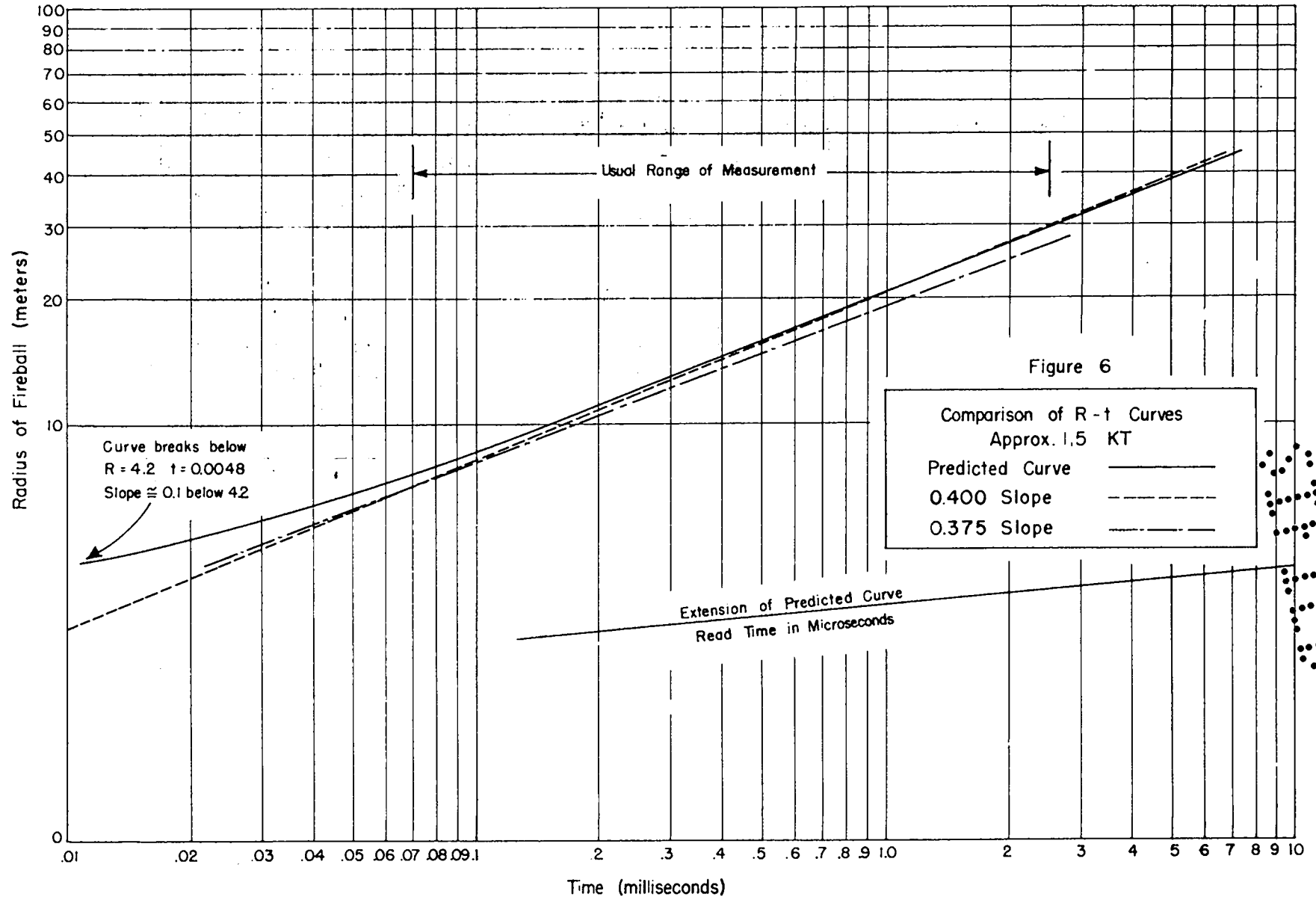
The variations in slope were investigated in greater detail by the definition that on a log-log plot, the slope, n , between points i and $i + 1$ is

$$n = \frac{\log R_{i+1} - \log R_i}{\log t_{i+1} - \log t_i}$$

From this, it follows as usual that



SECRET



$$\frac{R_{i+1}}{R_i} = \left(\frac{t_{i+1}}{t_i} \right)^n$$

The values are tabulated in Columns 6, 7, and 8 of Table 2. The values of n are plotted in Fig. 7. A semi-log plot is used to obtain a properly weighted conception of the average slope on a log-log plot. Figure 7 again is in excellent agreement with the observed results from Sandstone. Over the usual range of measurement, the average value of the predicted curve is

$$\bar{n} \approx 0.377,$$

in comparison with the observed value of

$$0.374 \pm 0.005 .$$

The comparison is quite arbitrary. For fireball measurements at relatively large radii, slopes close to 0.4 should be observed; for measurements restricted to small radii, much smaller slopes would be observed.

3. DISCUSSION

3.1 Qualitative Description of Results

The foregoing analysis leaves little question that the deviation from the 0.4 law, as observed at Sandstone, is indeed a real variation. In fact, one should recognize about four distinct zones on the radius-time plot, using as an example 1.5 kt.

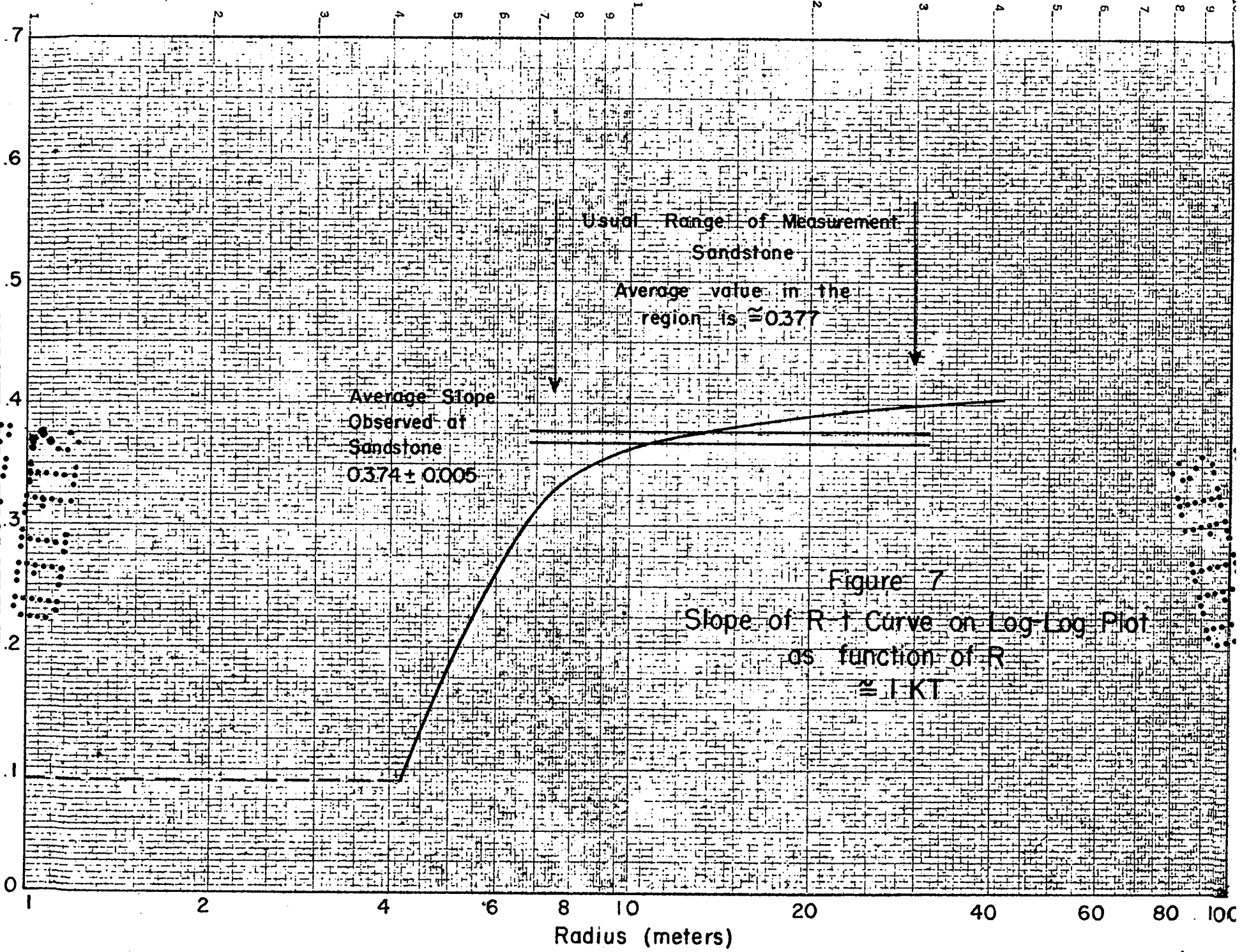


Figure 7
Slope of R-1 Curve on Log-Log Plot
as function of R
 $\approx 1/KT$

Average Slope
Observed at
Sandstone
 0.374 ± 0.005

Usual Range of Measurement
Sandstone
Average value in the
region is ≈ 0.377



(1) Region of low radii, less than 4.2 meters, where strong shock does not apply at all. A radiation model would predict very flat slopes, approximately 0.1, although even this may be distorted because we have neglected the finite size of the bomb case in this region.

(2) A transition zone between radii of 4.2 and about 8 meters, where the slope changes rapidly, due to the influence of the early phase and the influence of varying γ .

(3) The usual range of measurement, 8 to 30 meters, where a slight curvature persists, primarily due to the influence of a variable γ . In this region, an average slope of 0.375 has some meaning.

(4) Radii greater than 30 meters where the slope approaches 0.4, then rises again as the shock becomes too weak for strong shock theory to apply.

For bombs of other energies, the zones shift by the appropriate scaling factor.

3.2 Methods of Scaling

The analysis shows that no method of scaling is really trustworthy unless the comparison is made at equal pressure or equal values of some other state variable.

A suitable method would be as follows: Plot the radius-time curve as well as possible, perhaps using Fig. 7 as a guide. For several points on the curve, determine

$$U = n \frac{R}{t},$$





because this is the functional relation between U and the locally determined slope, n , on a log-log plot. On another sheet, plot the values of

$$\log \frac{U}{C_0} = \log \left(\frac{n}{C_0} \frac{R}{t} \right)$$

as a function of $\log R$, this because the actual invariant for different bombs is U/C_0 rather than U .

This same procedure will already be done for a bomb of known yield, with a comparison as in Fig. 8.

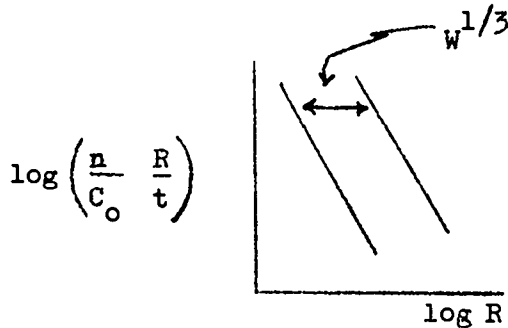
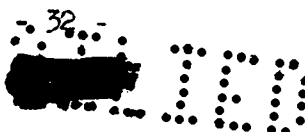


Fig. 8

The horizontal displacement between the two curves is, of course, the cube root of the yield ratio, $W^{1/3}$. The advantage of this method is that constant errors in time or distance will cancel out, as well as common differences in slope, so that a constant value of $W^{1/3}$ should be obtained. If a constant value for $W^{1/3}$ is not obtained, it indicates a failure of the scaling assumptions. In this type of plot, the



average slope will actually be quite close to - 1.5, a slight curvature resulting from the influence of variable γ on U , but avoiding the integrated S-shaped displacement of Fig. 3.

This particular method has a further advantage in that the "free-air" pressure may be readily deduced from this plot. From strong shock theory with variable γ , the pressure corresponding to

$$\frac{U}{C_0} = \frac{n}{C_0} \frac{R}{t}$$

is readily deduced. By this simple transformation of the ordinate, Fig. 8 becomes a familiar peak pressure vs distance curve. The corresponding analytic procedure is as follows.

Since

$$\frac{U}{C_0} = \sqrt{\frac{\gamma + 1}{2\gamma_0}} (\xi - 1)^{1/2},$$

and

$$\xi - 1 = \frac{A}{R^3},$$

it follows that the locally determined constant, K , in the $\log U/C_0$ vs $\log R$ plot is actually

$$K = \sqrt{\frac{\gamma + 1}{2\gamma_0}} A^{1/2},$$

from which A is readily derived as

$$A = \frac{2\gamma_0}{\gamma + 1} K^2$$

When the variations in slope or in C_0 are observed to be small, a useful procedure for drawing a radius-time curve would be to make a tracing of the predicted curve in Fig. 7 and plot the observed points on log-log paper of the same functional modulus. Superimpose the two papers, drawing a 45° line on each. Next, shift the tracing paper along the 45° line until a best fit is obtained for the observed points. The analysis in this paper may not be sufficiently rigorous to give an exact fit in all cases, but it would indicate where curvature is most severe and assist in a more intelligent weighting of the experimental points. If an average slope is used, a procedure such as this must be used to keep the average slope from varying with the range of measurement. If the work is carefully done, the lateral or vertical displacement is, of course, $W^{1/3}$.

3.3 Predictions from Theory

If very early photographs are obtained,

$$R < \frac{5}{W^{1/3}},$$

these should show radii very much greater than the 0.4 law would predict, and considerably higher than even the 0.375 law. (See Fig. 9.)

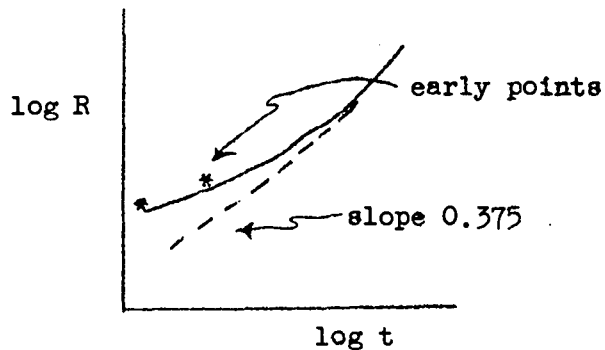


Fig. 9

Every effort should be made to correlate these points because they will considerably clarify the details of the early "radiative phase" and perhaps the point at which strong shock theory becomes applicable.

If an R-t plot of high explosive (HE) is made, one might expect slopes very much closer to the 0.4 law, because of the absence of a "radiative phase", although here the relatively long duration of energy formation in HE will have to be considered.

3.4 Elaboration of the Present Paper

It is recognized that some parts of the derivation may warrant more careful consideration.

3.4.1 Early Phase

A more careful investigation of the early phase of fireball growth is warranted, correlated where possible by such



measurements at low radii as can be obtained. Even without the model of a "radiative phase", strong shock theory is questionable because of the finite mass of the bomb in comparison with that of air already enveloped. For a 50-kt bomb, where the bomb parts are of the order of 5×10^6 grams, a critical radius would be that of an equivalent mass of air, which is

$$r = \left(\frac{5 \times 10^6}{\frac{4}{3} \pi \rho} \right)^{1/3}$$

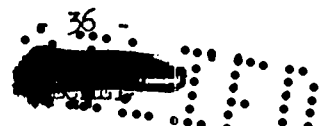
$$\rho \text{ for air} = 1.29 \times 10^{-3} \text{ gms/cm}^3,$$

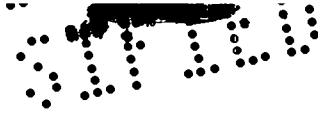
$$r = \left(\frac{5 \times 10^6}{\frac{4\pi}{3} 1.3 \times 10^{-3}} \right)^{1/3} = 10 \text{ meters.}$$

The corresponding transition range from our model is

$$r = \left(\frac{50}{1.5} \right)^{1/3} \times 4.2 = 13 \text{ meters.}$$

This is a situation where the core of the shock wave is much more dense than the outer zone, far from having the good "Taylor similarity" required. A careful investigation of mass effects during the early phase could lead to the same result as the "radiative phase" model in distorting the R-t curve at later times.





The results from Ranger should considerably clarify this point. If mass effects are important, they will show up as a failure of scaling at small radii for bombs of low yield.

At very small radii, the equations used were of the form

$$R = c t^n .$$

To be strictly true, $R \approx 0.5$ at $t \approx 0$, when the explosion breaks through the case. For this reason, the initial slopes would be different from 0.9, but this is probably a trivial point at radii of interest.

3.4.2 Similarity Consideration

The assumption was made in this paper that

$$P \sim \frac{1}{R^3} .$$

Previous work by the author on rapid integrations of wave forms has indicated that the density distribution behind a shock front is strongly dependent on γ . The point is too lengthy to elaborate here, but it may be sufficient to recall that for strong shocks the peak shock density is given by

$$\rho_s = \rho_0 \frac{\gamma + 1}{\gamma - 1} .$$

It can also be shown that when the shock front is at R , with density ρ_s , the density at r behind the shock is





$$\rho \approx \rho_0 \left(\frac{r}{R} \right)^{(6/\gamma-1)}$$

As a result, the density distribution behind the shock is markedly perturbed in regions where γ is rapidly varying. Temperatures and entropy are similarly affected, and there is reasonable question whether or not similarity laws strictly apply.

The rather remarkable correlation between the predicted curve and the Sandstone results is some assurance that the deviations caused by a failure of similarity are small.

3.4.3 Applicability of the Rankine-Hugoniot Equations

The strong shock theory used here assumed that the air immediately in front of the shock was at constant ambient conditions. During the shock, some radiation is obviously escaping from the luminous front, because this is the process by which one observes the fireball. The radiation leaving the fireball has a spectral distribution, so that short wavelengths may be rapidly absorbed in air just ahead of the shock and longer wavelengths may completely escape. As a consequence, the pressure distribution might be as indicated in Fig. 10.



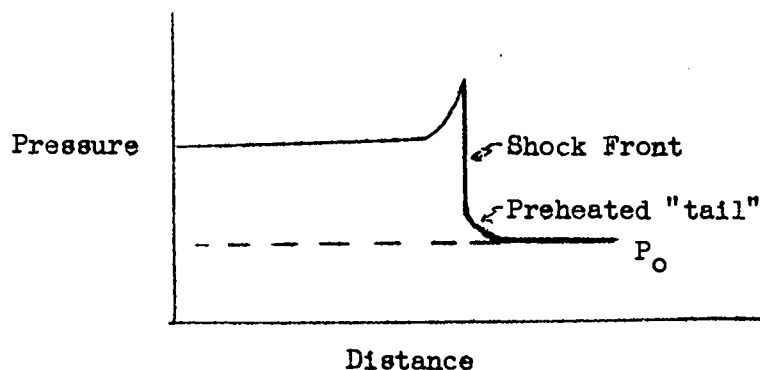


Fig. 10

The point was not raised because it is believed that the Rankine-Hugoniot equations apply just as well across the preheated "tail" as across the shock. If the tail existed, and all conditions just ahead of the shock were precisely known, these would lead to the same result as the assumptions made. It is possible, however, that the loss of radiant energy at the shock front could appreciably affect the velocity and, hence, the R-t curve.

3.4.4 Correction of Observed Results

It had been suggested that the deviation from the 0.4 law was accounted for by halation of the photographic film during the initial periods of intense brightness, with subsequently less halation as the fireball grew. The findings in the present paper by no means preclude the necessity for applying such corrections and, in fact, may make these small corrections more meaningful.

4. CONCLUSIONS

The following conclusions appear justified.

(a) The log R - log t plot describing the growth of a fireball from an atomic bomb should have a variable slope, between 0.1 and 0.4, depending on the actual range of measurement.

(b) The observed slope of 0.374 ± 0.005 at Sandstone is consistent with the theory over the range of measurements made.

(c) Any rigorous method of scaling must demand that comparisons be made only at points where hydrodynamic variables are equal.

(d) More careful investigation of the very early phases of growth is warranted to improve the present predicted curve and to determine more precisely where and to what degree scaling can be expected to fail.

UNCLASSIFIED

APPENDIX ACOMPARISON OF FIREBALL GROWTH AND PEAK-PRESSURE MEASUREMENTS

The value of A in

$$P = \frac{WA}{R^3}$$

was roughly determined from Sandstone fireball data which gave

$$R = c t^{0.374}$$

$$\frac{U}{C_0} = \frac{n}{C_0} \frac{R}{t} = \frac{1}{\sqrt{2\gamma_0}} (\xi - 1)^{1/2} (\gamma + 1)^{1/2}$$

$$= \frac{1}{\sqrt{2\gamma_0}} \frac{A^{1/2}}{R^{3/2}} (\gamma + 1)^{1/2}$$

$$A^{1/2} = \frac{n}{C_0} \frac{R}{t} \frac{\sqrt{2\gamma_0}}{(\gamma + 1)^{1/2}} R^{3/2}$$

$$A = \frac{n^2}{C_0^2} \frac{R^5}{t^2} \frac{2\gamma_0}{\gamma + 1} = \frac{n^2}{C_0^2} c^5 \frac{2\gamma_0}{\gamma + 1}$$

UNCLASSIFIED

UNCLASSIFIED

The average value of sound velocity from X-Ray, Yoke and Zebra, scaled to 50 kt, is $C = 41.9 \text{ meters/sec}^{0.374}$. Ambient sound velocity is taken as $C_0 = 1140 \text{ ft/sec} = 0.345 \text{ meters/msec}$. From an estimate of the peak pressures in the Sandstone fireballs, a representative value for γ is 1.2.

$$A = \frac{(0.374)^2}{(0.345)^2} (41.9)^5 \left(\frac{2.8}{2.2} \right)$$

$$= 1.94 \times 10^8 \text{ for 50 kt}$$

$$= 3.9 \times 10^6 \text{ for 1 kt.}$$

This value constitutes a rough prediction for the expected results of a measurement of free air pressure from an atomic bomb.

The methods used in this paper are also applicable to correlating fireball measurements with measured reflected pressures to obtain reflection factors, or similarly, with extrapolation of free-air pressure measurement at a lower pressure. A calculation from C. W. Lampson's fit of the Bikini-Able peak-pressure data gives, for 1 kt,

$$A = 3.7 \times 10^6 .$$

This is in fair agreement with the value of $A = 3.9 \times 10^6$ from fireball data, but is not to be taken literally because of other factors which have not been considered: reflection factors in the region of

UNCLASSIFIED

UNCLASSIFIED

Mach reflection, surface energy losses, energy retained in the fireball and not appearing as blast, and because Lampson used horizontal instead of radial distances. Most of these can be resolved: from the work of LA-743R, Bikini-Able data were fitted to TNT results after reflection factors were applied. A reflection factor of 1.5 was assumed to be applicable at great distances, and to fit the curve another correction factor of $3/4$ was found necessary. This means that to fit a free-air TNT curve (as Lampson did) to an atomic bomb requires a combined factor of

$$K = \frac{3}{4} \times \frac{3}{2} = \frac{9}{8} ,$$

that is, the "A" in the reflected pressure region should be $9/8$ of the "A" from fireball measurements. The actual ratio here is more like $8/9$.

The work of LA-743R also showed that the reflected pressure vs horizontal distance was a curve of the form

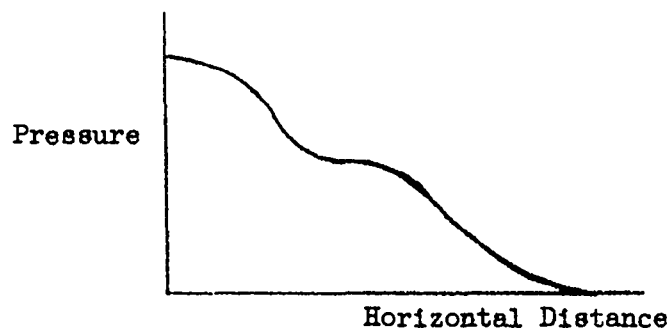


Fig. A 1

Reflected Pressure vs Horizontal Distance

UNCLASSIFIED


UNCLASSIFIED

The attempt to fit data of this form, even in the region beyond Mach reflection, with an equation like

$$P = \frac{A}{R^3} + \frac{B}{R^2} + \frac{C}{R}$$

as in Lampson's fit. would lead to low results for the coefficient A, as we have already found.

UNCLASSIFIED

44 15

DOCUMENT ROOM

REC. FROM *J. A.*

DATE *4/16/51*

REC. NO. REC. _____

44 15